

J.-L. Martin · A. Migus

G. A. Mourou · A. H. Zewail (Eds.)

Ultrafast Phenomena VIII

Proceedings

of the 8th International Conference,

Antibes Juan-Les-Pins, France, June 8–12, 1992

With 523 Figures

Springer-Verlag

Berlin Heidelberg New York

London Paris Tokyo

Hong Kong Barcelona

Budapest

Contents

Part I	Overview and General Prospects	
---------------	---------------------------------------	--

Additive Pulse Modelocking and Kerr-Lens Modelocking By H.A. Haus (With 6 Figures)	3
Molecular Control Spectrometer By Y. Yan, B.E. Kohler, R.E. Gillilan, R.M. Whitnell, K.R. Wilson, and S. Mukamel	8
Internal Motions of Proteins By M. Karplus	13
Some Theoretical Aspects of Electron Transfer in Supermolecules By J. Jortner and M. Bixon (With 3 Figures)	15
Femtosecond Time-Resolved Spectroscopy of Magneto-Excitons By D.S. Chemla, J.B. Stark, and W.H. Knox (With 6 Figures)	21
High-Order Harmonic Generation in Strong Laser Fields By A. L'Huillier and P. Balcou (With 3 Figures)	29
QED at 10^{20} W/cm ² By A.C. Melissinos (With 6 Figures)	34

Part II	Elementary Dynamics: Chemistry, Biology and Physics	
----------------	--	--

Femtochemistry By A.H. Zewail (With 6 Figures)	43
Transient Dichroism Studies of I ₂ Predissociation in Solution By N.F. Scherer, L.D. Ziegler, D. Jonas, and G.R. Fleming (With 3 Figures)	49
Investigation of the Primary Event in Vision Using 10 fs Blue-Green Optical Pulses By R.W. Schoenlein, L.A. Peteanu, Q.W. Wang, R.A. Mathies, and C.V. Shank (With 3 Figures)	53

Mechanisms of Charge Separation in Bacterial Reaction Centers By M.H. Vos, F. Rappaport, J.-C. Lambry, C. Rischel, J. Breton, and J.-L. Martin (With 2 Figures)	58
Coherent Phonons in Superconducting Materials By W. Albrecht, Th. Kruse, and H. Kurz (With 3 Figures)	63
Displacive Excitation of Coherent Phonons By T.K. Cheng, J. Vidal, H.J. Zeiger, E.P. Ippen, G. Dresselhaus, and M.S. Dresselhaus (With 1 Figure)	66
Femtosecond Time-Resolved Photodissociation of Triiodide Ions in Alcohol Solution: Directly Observed Photoinduced Vibrational Coherence of Reactants and Products By U. Banin, A. Waldman, and S. Ruhman (With 4 Figures)	68
Vibrational Coherence in Charge Transfer By K. Wynne, C. Galli, P.J.F. De Rege, M.J. Therien, and R.M. Hochstrasser (With 1 Figure)	71
Ultrafast Dynamics in Solution: Wavepacket Motion and the Cage Effect in Iodine By Y. Yan, R.M. Whitnell, K.R. Wilson, and A.H. Zewail (With 1 Figure)	74
Femtosecond Time-Resolved Ionization Spectroscopy of Polyatomic Molecules By M. Seel and W. Domcke (With 1 Figure)	76
A Study of Nuclear Vibrational Wave Packets in Na ₂ by Time- and Frequency-Resolved Fluorescence Upconversion By I.A. Walmsley, T.J. Dunn, J. Sweetser, and C. Radzewicz (With 3 Figures)	78
Ultrafast Dynamics of Solid C ₆₀ By S.L. Dexheimer, D.M. Mittleman, R.W. Schoenlein, W. Vareka, X.-D. Xiang, A. Zettl, and C.V. Shank (With 2 Figures)	81
Femtosecond Dynamics of Molecular and Cluster Ionization and Fragmentation By T. Baumert, R. Thalweiser, V. Weiß, and G. Gerber (With 5 Figures)	83
Dephasing and Beats of Excitonic-Enhanced Transitions of J-Aggregates Measured by Femtosecond Time-Resolved Resonance CARS By V.F. Kamalov, R. Inaba, and K. Yoshihara (With 1 Figure)	87
Excited States Dynamics of the Special Pair Dimer By P.O.J. Scherer and S.F. Fischer (With 4 Figures)	89
Creation of an Anti-Wavepacket in a Rydberg Atom By L.D. Noordam, H. Stapelfeldt, D.I. Duncan, and T.F. Gallagher (With 3 Figures)	92

Squeezing of the Molecular Vibrations by Femtosecond Laser Pulses By A.V. Vinogradov and J. Janszky (With 1 Figure)	95
--	----

Part III Spectroscopy and Advances in Measurements

Spectroscopic Applications of Phase-Locked Femtosecond Pulses By N.F. Scherer, M. Cho, L.D. Ziegler, M. Du, A. Matro, J. Cina, and G.R. Fleming (With 5 Figures)	99
Use of Piecewise Phase-Swept Pulses to Counteract Inhomogeneous Decay in Wave Packet Interferometry By L.W. Ungar, A. Matro, and J.A. Cina (With 1 Figure)	105
Ultrafast Nonlinear Spectroscopy with Chirped Optical Pulses By E.T.J. Nibbering, F. de Haan, D.A. Wiersma, and K. Duppen (With 2 Figures)	107
Multiple Excitation Pulse, Multiple Probe Pulse Femtosecond Spectroscopy By G.P. Wiederrecht, W. Wang, K.A. Nelson, A.M. Weiner, and D.E. Leaird (With 2 Figures)	110
Stimulated Emission Pumping and Selective Excitation by Adiabatic Passage with Frequency-Modulated Picosecond Laser Pulses By J.S. Melinger, A. Hariharan, S.R. Gandhi, and W.S. Warren (With 2 Figures)	113
A Subpicosecond Optical Sampling System By J.D. Kafka, J.W. Pieterse, and M.L. Watts (With 2 Figures)	116
Femtosecond Sagnac Interferometry By J.-C. Diels, P. Dorn, M. Lai, W. Rudolph, and X.M. Zhao (With 3 Figures)	120
Femtosecond Time-Gated Imaging of Translucent Objects Hidden in Highly Scattering Media By K.M. Yoo, B.B. Das, F. Liu, Q. Xing, and R.R. Alfano (With 2 Figures)	124
Femtosecond Waveform Processing via Spectral Holography By A.M. Weiner, D.E. Leaird, D.H. Reitze, and E.G. Paek (With 4 Figures)	128
The Chronocyclic Representation of Ultrashort Light Pulses By J. Paye (With 4 Figures)	133
Femtosecond Pulse Phase Measurement by Spectrally Resolved Up-Conversion By J.-P. Foing, J.-P. Likforman, and M. Joffre (With 3 Figures)	136

Single-Shot Measurement of the Intensity and Phase of a Femtosecond Pulse By D.J. Kane and R. Trebino (With 4 Figures)	138
Two-Photon Interference Measurement of Ultrafast Laser Pulses By M. Matsuoka, Y. Miyamoto, T. Kuga, M. Baba, and Y. Li (With 2 Figures)	140
Picosecond Single-Shot Pulse-Shape Measurement by Stochastic Sampling of Detected Photon Times By N. Adams, C. Bovet, E. Rossa, and A. Simonin (With 1 Figure)	142
Integrated Devices for Single Picosecond Pulse Measurements By V. Gerbe, M. Cuzin, M.C. Gentet, and J. Lajzerowicz (With 3 Figures)	145
The C850X Ultrafast Streak Camera: An Instrument to Study Spatially and Temporally Subpicosecond Laser–Matter Interaction By A. Mens, R. Sauneuf, D. Schirmann, R. Verrecchia, P. Audebert, J.C. Gauthier, J.P. Geindre, A. Antonetti, J.P. Chambaret, G. Hamoniaux, and A. Mysyrowicz (With 2 Figures)	147
Distortion of a 6 fs Pulse in the Focus of a BK7 Lens By Zs. Bor and Z.L. Horváth (With 1 Figure)	150

Part IV Tools: Sources and Amplifiers

Modelocking, Stabilizing, and Starting Ultrashort Pulse Lasers By E.P. Ippen (With 4 Figures)	155
17 fs Pulses from a Mode-Locked Ti:Sapphire Laser By C.P. Huang, M.T. Asaki, S. Backus, H. Nathel, H.C. Kapteyn, and M.M. Murnane (With 2 Figures)	160
Design Considerations for Femtosecond Ti:Sapphire Oscillators By Ch. Spielmann, P.F. Curley, T. Brabec, E. Wintner, A.J. Schmidt, and F. Krausz (With 3 Figures)	163
Self-Mode-Locked Cr ³⁺ :LiCaAlF ₆ and Cr ³⁺ :LiSrAlF ₆ Lasers By A. Miller, P. Li Kam Wa, B.H.T. Chai, J.M. Evans, and W. Sibbett (With 2 Figures)	166
Sub-50 fs Pulse Generation from a Self-Starting CW Passively Mode-Locked Cr:LiSrAlF ₆ Laser By N.H. Rizvi, P.M.W. French, and J.R. Taylor (With 2 Figures)	169
CW Krypton-Laser Pumped Cr ³⁺ :LiSrAlF ₆ and Cr ³⁺ :LiSr _{0.8} Ca _{0.2} AlF ₆ Crystals Produce 150 fs Mode-Locked Pulses By A. Miller, P. Li Kam Wa, H.S. Wang, S.L. Ayres, E.W. Van Stryland, and B.H.T. Chai (With 3 Figures)	172

60-fs Chromium-Doped Forsterite ($\text{Cr}^{4+}:\text{Mg}_2\text{SiO}_4$) Laser By A. Seas, V. Petričević, and R.R. Alfano (With 3 Figures)	174
Femtosecond Pulses from Nd:Glass Lasers By A.J. Schmidt, M.H. Ober, M. Hofer, M.E. Fermann, F. Krausz, T. Brabec, Ch. Spielmann, and E. Wintner (With 3 Figures)	177
A Diode-Pumped Picosecond Oscillator at 1053 nm By I.P. Mercer, Z. Chang, M.R.G. Miller, C.N. Danson, C.B. Edwards, and M.H.R. Hutchinson (With 3 Figures)	182
A New Intracavity Antiresonant Semiconductor Fabry-Perot Passively Mode-Locks Nd:YLF and Nd:YAG Lasers By U. Keller, D.A.B. Miller, G.D. Boyd, T.H. Chiu, J.F. Ferguson, and M.T. Asom (With 3 Figures)	184
CW Mode-Locked Singly-Resonant Optical Parametric Oscillator Pumped by a Ti:Sapphire Laser By A. Nebel, U. Socha, and R. Beigang (With 1 Figure)	187
70 fs, High-Average Power, CW Infrared Optical Parametric Oscillator By G. Mak, Q. Fu, and H.M. van Driel (With 2 Figures)	190
Femtosecond Intracavity Dispersion Measurements By W.H. Knox (With 2 Figures)	192
Time Synchronization Measurements Between Two Self-Modelocked Ti:Sapphire Lasers By D.E. Spence, W.E. Sleat, J.M. Evans, W. Sibbett, and J.D. Kafka (With 2 Figures)	194
Femtosecond Synchronous Pumping of Dye Lasers with <100 fs Jitter By W.H. Knox and F.A. Beisser (With 2 Figures)	196
Development of High Average Power Femtosecond Amplifiers Based on Ti-, Cr- and Nd:Doped Materials By J. Squier, S. Coe, G. Mourou, D. Harter, and F. Salin	198
Femtosecond Pulse Amplification and Continuum Generation at >250 kHz with a Ti:Sapphire Regenerative Amplifier By T.B. Norris (With 4 Figures)	200
Millijoule Femtosecond Pulse Amplification in $\text{Ti:Al}_2\text{O}_3$ at Multi-kHz Repetition Rates By F. Salin, J. Squier, G. Mourou, and G. Vaillancourt (With 4 Figures)	203
High Repetition Rate CW Pumped Cr:LiSAF Regenerative Amplifier By F. Balembois, P. Georges, F. Salin, G. Roger, and A. Brun (With 4 Figures)	206

18 fs Pulse Generation by a Single Excimer-Laser-Pumped Pulsed Dye Laser By P. Simon, C. Jordan, and S. Szatmari (With 2 Figures)	209
Monolithic CPM Diode Lasers By M.C. Wu, Y.K. Chen, T. Tanbun-Ek, and R.A. Logan (With 5 Figures)	211
Ultrashort Pulse Generation from High-Power Arrays Using Intracavity Nonlinearities By L.Y. Pang, J.G. Fujimoto, and E.S. Kintzer (With 3 Figures)	217
100-Gbps Response of Microcavity Lasers By H. Yokoyama, Y. Nambu, and T. Shimizu (With 2 Figures)	220
Sequential Laser Emission in Multiple Quantum Well Vertical-Cavity Structures By C. Tanguy, J.-L. Oudar, B. Sermage, and R. Azoulay (With 2 Figures)	222
Experimental Analysis of Gain Modulation in Sub-Picosecond (~ 0.45 ps) Mode-Locked Laser Diodes By N. Stelmakh, J.-M. Lourtioz, and D. Pascal (With 3 Figures)	224
Generation of Stable Pulse Trains with a Passively Modelocked Er-Fiber Laser By M.E. Fermann, M.J. Andrejco, Y. Silberberg, and A.M. Weiner (With 4 Figures)	227
Generation of Pairs of Solitons in an All-Fibre, Femtosecond Soliton Source By D.J. Richardson, V.V. Afanasjev, A.B. Grudinin, and D.N. Payne (With 5 Figures)	229
Nonlinear Loop Mirrors in Fiber Lasers By I.N. Duling III, C.J. Chen, P.K. Wai, and C.R. Menyuk (With 4 Figures)	232
Temporal Characteristics of the Ytterbium–Erbium Figure-8 Laser By I.Yu. Khrushchev, A.B. Grudinin, and E.M. Dianov (With 3 Figures)	235
Generation of 1.7 ps Solitons by Amplification of Pulses from a Laser Diode with Saturable Absorber in an Erbium-Doped Fibre By I.Yu. Khrushchev, A.B. Grudinin, E.M. Dianov, D.V. Kuksenkov, and E.L. Portnoy (With 3 Figures)	237

Part V High Intensity and Nonlinear Effects

Generation of Ultra-Intense Pulses and Applications By G. Mourou (With 1 Figure)	241
---	-----

Generation of 50 TW Femtosecond Pulses in a Nd-Glass Chain By C. Rouyer, E. Mazataud, I. Allais, A. Pierre, and S. Seznec (With 2 Figures)	248
All-Solid Femtosecond Oscillator–Amplifier Laser Chain with 100 mJ per Pulse By C. Le Blanc, G. Grillon, J.P. Chambaret, G. Boyer, M. Franco, A. Mysyrowicz, and A. Antonetti (With 1 Figure)	251
Development of a High Intensity Femtosecond LiSAF Laser By M.C. Richardson, P. Beaud, B.H.T. Chai, E. Miesak, Y.-F. Chen, and V. Yanovsky (With 2 Figures)	253
Contrasted Behaviors of Stark-Induced Resonances in Multiphoton Ionization of Krypton By E. Mevel, R. Trainham, J. Breger, G. Petite, P. Agostini, J.P. Chambaret, A. Migus, and A. Antonetti (With 1 Figure)	255
Phase-Dependent Ionization Using an Intense Two-Color Light Field By D. Schumacher, M.P. de Boer, H.G. Muller, R.R. Jones, and P.H. Bucksbaum (With 2 Figures)	257
Stabilization of Atoms in Ultra-Intense Laser Pulses: A Classical Model By A. Maquet, T. Ménis, R. Taïeb, and V. Véliard (With 1 Figure)	259
Inertially Confined Molecular Ions By M. Laberge, P. Dietrich, and P.B. Corkum (With 2 Figures)	261
A Femtosecond Lightning Rod By X.M. Zhao, C.Y. Yeh, J.-C. Diels, and C.Y. Wang (With 2 Figures)	264
Plasma Physics with Ultra-Short and Ultra-Intense Laser Pulses By T.W. Johnston, Y. Beaudoin, M. Chaker, C.Y. Côté, J.C. Kieffer, J.P. Matte, H. Pépin, C.Y. Chien, S. Coe, G. Mourou, and D. Umstadter (With 1 Figure)	267
X-Rays Generated by Femtosecond Laser-Produced Plasmas By J.P. Geindre, P. P. Audebert, A. Rousse, F. Fallières, J.C. Gauthier, A. Mysyrowicz, G. Grillon, J.P. Chambaret, A. Antonetti, A. Mens, R. Verrecchia, R. Sauneuf, and P. Schirman (With 2 Figures)	272
K-Shell Emission from 100 fs Laser-Produced Plasmas Created from Porous Aluminum Targets By R. Shepherd, D. Price, B. White, S. Gordan, A. Osterheld, R. Walling, D. Slaughter, and R. Stewart (With 2 Figures)	275
Kilovolt X-Ray Emission from Femtosecond Laser-Produced Plasmas By G. Jenke, H. Schüler, T. Engers, D. von der Linde, I. Uschmann, E. Förster, and K. Gäbel (With 1 Figure)	278

Ultrafast Spectroscopy of Plasmas Generated by Superintense Femtosecond Laser Pulses By D. von der Linde, H. Schüler, H. Schulz, and T. Engers (With 3 Figures)	280
Picosecond Soft-X-Ray Pulse Length Measurement by Pump–Probe Absorption Spectroscopy By M.H. Sher, U. Mohideen, H.W.K. Tom, O.R. Wood II, G.D. Aumiller, D.L. Windt, W.K. Waskiewicz, J. Sugar, T.J. McIlrath, and R.R. Freeman (With 4 Figures)	283
Photon Acceleration via Laser-Produced Ionization Fronts By R.L. Savage Jr., R.P. Brogle, W.B. Mori, and C. Joshi (With 5 Figures)	286
Propagation of Intense Laser Pulses in Plasmas By E. Esarey, P. Sprangle, J. Krall, and G. Joyce (With 1 Figure)	290
Ponderomotive Steepening in Short-Scale-Length Laser-Plasmas By D. Umstadter and X. Liu (With 2 Figures)	293
Possibility of Experimental Studies of Nonlinear Quantum Electrodynamics Effects Using High Power Ultrashort Laser Pulses By P.G. Kryukov (With 1 Figure)	296
Soliton-Like Self-Trapping of Three-Dimensional Patterns By A. Barthelemy, C. Froehly, M. Shalaby, P. Donnat, J. Paye, and A. Migus (With 9 Figures)	299
Physical Origins of the Spectral Continuum: Self-Focusing, Self-Trapping and Cerenkov Radiation By F. Salin, J. Watson, J.-F. Cormier, P. Georges, and A. Brun (With 2 Figures)	306
Diffraction and Focussing of Spectral Energy in a Two-Photon Process By B. Broers, L.D. Noordam, and H.B. van Linden van den Heuvell (With 3 Figures)	309
Efficient Raman Conversion of Femtosecond UV Light Pulses By K.A. Stankov and Y.-W. Lee (With 1 Figure)	311
Organic Crystalline Fiber for Efficient Compression of Femtosecond Laser Pulses By M. Yamashita (With 1 Figure)	313
Nonlinear Temporal Diffraction in Optical Fibers By G.R. Boyer, M.K. Jackson, J. Paye, M.A. Franco, and A. Mysyrowicz (With 3 Figures)	315
Generation of a Soliton Pulse Train in an Optical Fibre Using Two CW Single-Frequency Diode Lasers By S.V. Chernikov, J.R. Taylor, P.V. Mamyshev, and E.M. Dianov (With 2 Figures)	318

Experimental Investigation of Dark Solitons Interaction By Ph. Emplit, J.-P. Hamaide, and M. Haelterman (With 3 Figures)	320
Femtosecond Pulse Propagation in Erbium-Doped Single-Mode Fibers By J.M. Hickmann, A.S.L. Gomes, C.B. de Araújo, and A.S. Gouveia-Neto (With 3 Figures)	323
Compression of Pulses from Soliton Fibre Lasers in a Dispersion-Decreasing Fibre By S.V. Chernikov, D.J. Richardson, E.M. Dianov, and D.N. Payne (With 4 Figures)	325

Part VI Metals, Surfaces and Materials

Observation of the Thermalization of Electrons in a Metal Excited by Femtosecond Optical Pulses By W.S. Fann, R. Storz, H.W.K. Tom, and J. Bokor (With 2 Figures)	331
Femtosecond Thermionic Emission: Experiment, Analytical Theory, and Particle Simulations By M.C. Downer, D.M. Riffe, X.Y. Wang, J.L. Erskine, D.L. Fisher, T. Tajima, and R.M. More (With 2 Figures)	335
Electron–Electron Dynamics Observed in Femtosecond Thermoreflection Measurements on Noble Metals By R.H.M. Groeneveld, R. Sprik, and Ad. Lagendijk (With 2 Figures) . .	338
Inversion of Single- and Two-Photon Photoelectric Sensitivities of Metals in the Femtosecond Range By J.P. Girardeau-Montaut, C. Girardeau-Montaut, S.D. Moustazizis, and C. Fotakis (With 1 Figure)	340
Femtosecond Relaxation of Plasma Excitations in Silver Films By R.A. Höpfel, D. Steinmüller-Nethl, F.R. Aussenegg, and A. Leitner (With 3 Figures)	342
Femtosecond Free Induction Decay of Metal Surface Adsorbate Vibrations By J.C. Owrutsky, J.P. Culver, M. Li, Y.R. Kim, M.J. Sarisky, M.S. Yeganeh, R.M. Hochstrasser, and A.G. Yodh (With 1 Figure)	345
Observation of Laser-Induced Desorption of CO from Cu(111) with 100 fs Time-Resolution By J.A. Prybyla, H.W.K. Tom, and G.D. Aumiller (With 2 Figures)	347
Femtosecond Desorption of Molecular Oxygen from Pt(111) By F.-J. Kao, D.G. Busch, D. Gomes da Costa, D. Cohen, and W. Ho (With 1 Figure)	350

Femtosecond Carrier Dynamics in Solid C ₆₀ Films By S.D. Brorson, M.K. Kelly, U. Wenschuh, R. Buhleier, and J. Kuhl (With 4 Figures)	354
The Role of Covalency in Femtosecond Time-Resolved Reflectivity of Hydrodynamically Expanding Solid Surfaces By X.Y. Wang, H.Y. Ahn, and M.C. Downer (With 1 Figure)	357
Ultrafast Formation Processes of Self-Trapped Excitons in Alkali Iodide Crystals under Band-to-Band Excitation By T. Tokizaki, S. Iwai, T. Shibata, A. Nakamura, K. Tanimura, and N. Itoh (With 2 Figures)	360
Femtosecond Self-Trapping of Interacting Electron–Hole Pairs in α -SiO ₂ By W. Joosen, S. Guizard, P. Martin, G. Petite, P. Agostini, A. Dos Santos, G. Grillon, J.P. Chambaret, D. Hulin, A. Migus, and A. Antonetti (With 4 Figures)	362
Ultrafast Soft Mode Dynamics in Ferroelectric Crystals By G.P. Wiederrecht, T.P. Dougherty, and K.A. Nelson (With 3 Figures)	365
Temporal Domain Study of the Phase Transition in PbTiO ₃ : A ₁ Symmetry Investigation By D.P. Kien, J.C. Loulergue, and J. Etchepare (With 2 Figures)	368
Femtosecond Transient Absorption Measurements on Low Band Gap Thiophene Polymers By A. Cybo-Ottoné, M. Nisoli, V. Magni, S. De Silvestri, O. Svelto, G. Zerbi, and R. Tubino (With 2 Figures)	370
Effects of Crosslinking in Host Polymer on Picosecond Optical Dephasing of Doped Dye Molecules By S. Nakanishi, S. Fujiwara, M. Kawase, and H. Itoh (With 3 Figures)	372
Ultrafast Relaxation of Exciton and Soliton–Antisoliton Pair in One-Dimensional Conjugated Polymers By T. Kobayashi, M. Yoshizawa, S. Takeuchi, and A. Yasuda (With 2 Figures)	376
Polarization-Dependent Femtosecond Dynamics of MBE-Grown Phthalocyanine Organic Thin Films By Sandalphon, V.S. Williams, K. Meissner, N.R. Armstrong, and N. Peyghambarian (With 3 Figures)	379
Detection of a New Strongly-Coupled Vibration Mode During the Exciton Bleaching of Polydiacetylene By J.M. Nunzi, C. Hirlimann, and J.F. Morhange (With 1 Figure)	381

Pressure-Induced Vibrational Relaxation and Electronic Dephasing in Molecular Crystals By E.L. Chronister and R.A. Crowell (With 3 Figures)	384
Ultrafast Reversible Phase Changes for Optical Recording By J. Solfs, C.N. Afonso, F. Catalina, and C. Kalpouzos (With 1 Figure)	387
Picosecond Transient Absorption and Fluorescence Emission Studies of C ₆₀ and C ₇₀ in Solution By D. Kim, Y.D. Suh, S.K. Kim, and M. Lee (With 2 Figures)	389

Part VII Semiconductors, Confinement and Opto-Electronics

Transient Absorption-Edge Singularities in GaAs By D. Hulin, J.-P. Foing, M. Joffre, M.K. Jackson, J.-L. Oudar, C. Tanguy, and M. Combescot (With 3 Figures)	395
Nonthermal Distribution of Electrons in GaAs By D. Snoke and W.W. Rühle (With 1 Figure)	399
Femtosecond Carrier–Carrier Interaction in GaAs By T. Gong, K.B. Ucer, L.X. Zheng, G.W. Wicks, J.F. Young, P.J. Kelly, and P.M. Fauchet (With 4 Figures)	402
Quantum Beats versus Polarization Interference: An Experimental Distinction By M. Koch, J. Feldmann, G. von Plessen, E.O. Göbel, P. Thomas, and K. Köhler (With 1 Figure)	405
Plasmon–Phonon Coupling and Hot Carrier Relaxation in GaAs and Low-Temperature-Grown GaAs By R.I. Devlen, J. Kuhl, and K. Ploog (With 2 Figures)	408
Femtosecond Carrier–Carrier Interaction Dynamics in Doped GaAs By T. Furuta and A. Yoshii (With 1 Figure)	410
Femtosecond Carrier Kinetics in Low-Temperature-Grown GaAs By X.Q. Zhou, H.M. van Driel, A.P. Heberle, W.W. Rühle, and K. Ploog (With 2 Figures)	412
Transient Anisotropic Luminescence and Long-Living Polarization of an Optically Excited Dense Electron–Hole Plasma By A.L. Ivanov and H. Haug (With 2 Figures)	414
Hot Hole Capture by Shallow Acceptors in p-Type GaAs Studied by Picosecond Infrared Spectroscopy By A. Lohner, M. Woerner, T. Elsaesser, and W. Kaiser (With 2 Figures)	416

Ultrafast Dephasing and Interference of Coherent Phonons in GaAs By W. Kütt, T. Pfeifer, T. Dekorsy, and H. Kurz (With 2 Figures)	418
Femtosecond, Electronically-Induced Disorder of GaAs By J.-K. Wang, Y. Siegal, P.N. Saeta, N. Bloembergen, and E. Mazur (With 2 Figures)	420
Laser-Induced Ultrafast Order–Disorder Transitions in Semiconductors By K. Sokolowski-Tinten, J. Bialkowski, and D. von der Linde (With 1 Figure)	422
Femtosecond Carrier Dynamics in InGaAsP Optical Amplifiers By J. Mark and J. Mørk (With 1 Figure)	424
Ultrafast Nonlinear Refraction in Semiconductor Laser Amplifiers By M. Sheik-Bahae and E.W. Van Stryland (With 3 Figures)	426
Femtosecond Luminescence Spectroscopy of Indium Phosphide By E. Fazio and G.M. Gale (With 2 Figures)	429
Dynamics of Excitons Probed by Accumulated Photon Echo By T. Bouma, P. Vledder, and J.I. Dijkhuis (With 1 Figure)	431
Time-Resolved Measurement of Hot Carrier Cooling Rates in a-Si:H and a-Ge:H By M. Wraback and J. Tauc (With 2 Figures)	433
Dephasing of the Short Exciton–Polariton Pulses in Polar Semiconductors: The Cuprous Chloride Case By F. Vallée, F. Bogani, and C. Flytzanis (With 3 Figures)	435
Femtosecond Electronic Dynamics of CdSe Nanocrystals By C.V. Shank, R.W. Schoenlein, D.M. Mittleman, J.J. Shiang, and A.P. Alivisatos (With 4 Figures)	438
Quantum Beats Spectroscopy of Exciton Spin Dynamics in GaAs Heterostructures By S. Bar-Ad and I. Bar-Joseph (With 3 Figures)	443
Evidence of Slow Hole Spin Relaxation in n-Modulation Doped GaAs/AlGaAs Quantum Well Structures By Ph. Roussignol, P. Rolland, R. Ferreira, C. Delalande, G. Bastard, A. Vinattieri, J. Martinez-Pastor, L. Carraresi, M. Colocci, J.F. Palmier, and B. Etienne (With 1 Figure)	446
Femtosecond Time-Resolved Four-Wave Mixing in GaAs Quantum Wells By D.S. Kim, J. Shah, T.C. Damen, J.E. Cunningham, W. Schäfer, and S. Schmitt-Rink (With 4 Figures)	448
Exciton Radiative Lifetimes in GaAs Quantum Wells By R. Eccleston, J. Kuhl, W.W. Rühle, and K. Ploog (With 2 Figures)	451

Optical Investigation of Bloch Oscillations in a Semiconductor Superlattice By J. Feldmann, K. Leo, J. Shah, D.A.B. Miller, J.E. Cunningham, T. Meier, G. von Plessen, P. Thomas, and S. Schmitt-Rink (With 5 Figures)	454
Coherent Pulse Breakup in Femtosecond Pulse Propagation in Semiconductors By P.A. Harten, A. Knorr, S.G. Lee, R. Jin, F. Brown de Colstoun, E.M. Wright, G. Khitrova, H.M. Gibbs, S.W. Koch, and N. Peyghambarian (With 1 Figure)	458
Absorption Saturation of the Urbach's Tail in Multiple Quantum Wells By R. Raj, B.G. Sfez, D. Pellat, and J.L. Oudar (With 2 Figures)	460
Photon Echo Polarisation Rules in GaAs Quantum Wells By R. Eccleston, D. Bennhardt, J. Kuhl, P. Thomas, and K. Ploog (With 3 Figures)	463
Observation of Many-Body Effects in the Femtosecond Temporal Profile of Quasi-2D Exciton Free-Induction Decay By S. Weiss, M.-A. Mycek, J.-Y. Bigot, S. Schmitt-Rink, and D.S. Chemla (With 3 Figures)	466
Radiative Recombination of Free Excitons in GaAs Quantum Wells By B. Sermage, K. Satzke, C. Dumas, N. Roy, B. Deveaud, F. Clerot, and D.S. Katzer (With 4 Figures)	472
Field-Enhanced GaAs/AlGaAs Waveguide Saturable Absorbers By J.R. Karin, D.J. Derickson, R.J. Helkey, J.E. Bowers, and R.L. Thornton (With 2 Figures)	475
Picosecond Excitonic Nonlinearities in the Presence of Disorder By S.T. Cundiff and D.G. Steel (With 3 Figures)	478
Fast Optical Nonlinearities in Semiconductor Quantum Dots By G. Tamulaitis, R. Baltramiejūnas, S. Pakalnis, and A.I. Ekimov (With 2 Figures)	482
Terahertz Radiation from Coherent Electron Oscillations in a Double-Quantum-Well Structure By H.G. Roskos, M.C. Nuss, J. Shah, K. Leo, D.A.B. Miller, S. Schmitt-Rink, and K. Köhler (With 3 Figures)	484
Optical Generation of Terahertz Pulses from Polarized Excitons in Quantum Wells By P.C.M. Planken and M.C. Nuss (With 3 Figures)	487
Generation of High-Power Single-Cycle Picosecond Radiation By D.R. Dykaar, R.R. Jones, D. You, D. Schumacher, and P.H. Bucksbaum (With 3 Figures)	490

Transient Electron Transport in GaAs Quantum Wells: From the Ballistic to the Quasi-Equilibrium Regime By W. Sha, J. Rhee, and T.B. Norris (With 4 Figures)	493
A Novel Free-Standing Absolute-Voltage Probe with 2.3-Picosecond Resolution and 1-Microvolt Sensitivity By J. Kim, S. Williamson, J. Nees, and S. Wakana (With 3 Figures)	496
Picosecond Pseudomorphic AlGaAs/InGaAs MODFET Large-Signal Switching Measured by Electro-Optic Sampling By M.K. Jackson, M.Y. Frankel, J.F. Whitaker, G.A. Mourou, D. Hulin, A. Antonetti, M. Van Hove, W. De Raedt, P. Crozat, and H. Hafidallah (With 3 Figures)	500
Ultrafast Decay of Photodiffractive Gratings in Hetero n-i-p-i's by Enhanced In-Plane Transport By A.L. Smirl, D.S. McCallum, A.N. Cartwright, X.R. Huang, T.F. Boggess, and T.C. Hasenberg (With 2 Figures)	503
Picosecond High-Sensitivity $\text{In}_x\text{Ga}_{1-x}\text{As}$ Photodetectors By S. Gupta, J.F. Whitaker, S.L. Williamson, P. Ho, J.S. Mazurowski, and J.M. Ballingall (With 2 Figures)	505
An Ultrafast Polarization-Independent All-Optical Demultiplexer Utilizing Induced-Frequency Shift By T. Morioka, K. Mori, and M. Saruwatari (With 2 Figures)	508
Electrical Soliton Devices as >100 GHz Signal Sources By E. Carman, M. Case, M. Kamegawa, R. Yu, K. Giboney, and M. Rodwell (With 2 Figures)	511
Determination of Photonic Band Gaps and Dispersion in Two-Dimensional Dielectric Arrays with Ultrafast Electromagnetic Transients By W.M. Robertson, G. Arjavalingam, R.D. Meade, K.D. Brommer, A.M. Rappe, and J.D. Joannopoulos (With 2 Figures)	513

Part VIII **Biology: Primary Dynamics,
Electron and Energy Transfer**

Ultrafast Infrared Spectroscopy of Protein Dynamics By R.M. Hochstrasser, R. Diller, S. Maiti, T. Lian, B. Locke, C. Moser, P.L. Dutton, B.R. Cowen, and G.C. Walker (With 5 Figures)	517
Ultrafast Near-IR Spectroscopy of Carbonmonoxymyoglobin: The Dynamics of Protein Relaxation By M. Lim, T.A. Jackson, and P.A. Anfinrud (With 4 Figures)	522

Energetics and Dynamics of Global Protein Motion By R.J.D. Miller, J. Deak, S. Palese, M. Pereira, L. Richard, and L. Schilling (With 2 Figures)	525
Investigation of the Reaction Coordinate for Ligand Rebinding in Photoexcited Hemeproteins Using Transient Raman Spectroscopy By H. Zhu, R. Lingle, Jr., X. Xu, and J.B. Hopkins (With 2 Figures)	528
Resonance Raman Studies of Electronic and Vibrational Relaxation Dynamics in Heme Proteins By P.M. Champion, J.T. Sage, and P. Li	533
Molecular Processes in the Primary Reaction of Photosynthetic Reaction Centers By W. Zinth, C. Lauterwasser, U. Finkle, P. Hamm, S. Schmidt, and W. Kaiser (With 3 Figures)	535
Femtosecond Spontaneous Emission Studies of Photosynthetic Bacterial Reaction Centers By S.J. Rosenthal, M. Du, X. Xie, T.J. DiMaggio, M.E. Schmidt, J.R. Norris, and G.R. Fleming (With 1 Figure)	539
Subpicosecond Emission Studies of Bacterial Reaction Centers By P. Hamm and W. Zinth (With 1 Figure)	541
Picosecond Fluorescence Kinetics of Purple Bacterial Reaction Centers By M.G. Müller, K. Griebenow, and A.R. Holzwarth (With 2 Figures) . .	543
Primary Radical Pair Formation in Photosystem-Two Reaction Centres By D.R. Klug, J.R. Durrant, G. Hastings, Q. Hong, D.M. Joseph, J. Barber, and G. Porter (With 3 Figures)	546
Energy Transfer and Primary Charge Separation in Heliobacteria by Picosecond Transient Absorption Spectroscopy By P.I. van Noort, T.J. Aartsma, and J. Amesz (With 3 Figures)	549
Excitation Energy Transfer in Mutants of <i>Rb. sphaeroides</i> : The Effects of Changes in the Core Antenna Size By L.M.P. Beekman, R.W. Visschers, K.J. Visscher, B. Althuis, W. Barz, D. Oesterhelt, V. Sundström, and R. van Grondelle (With 3 Figures)	552
Femtosecond Excitation Transfer in Allophycocyanin By A.V. Sharkov, E.V. Khoroshilov, I.V. Kryukov, P.G. Kryukov, T. Gillbro, R. Fischer, and H. Scheer (With 1 Figure)	555
Femtosecond Förster Energy Transfer over 20 Å in Phycoerythrocyanin (PEC) Trimers By L.O. Palsson, T. Gillbro, A. Sharkov, R. Fischer, and H. Scheer (With 1 Figure)	557

Ultrafast Energy Transfer Within the Light-Harvesting Antenna of Photosynthetic Purple Bacteria By K.J. Visscher, V. Gulbinas, R.J. Cogdell, R. van Grondelle, and V. Sundström (With 2 Figures)	559
Femtosecond Dynamics in Rhodopsin By T. Kobayashi, M. Taiji, K. Bryl, M. Nakagawa, and M. Tsuda (With 2 Figures)	562
Subpicosecond Time-Resolved Spectroscopy of Halorhodopsin and Comparison with Bacteriorhodopsin By H. Kandori, K. Yoshihara, H. Tomioka, H. Sasabe, and Y. Shichida (With 3 Figures)	566
<hr/>	
Part IX	Chemistry: Electron and Energy Transfer, and Solvation Dynamics
<hr/>	
Femtosecond Intermolecular Electron Transfer: Dye in Weakly Polar Electron-Donating Solvent By K. Yoshihara, A. Yartsev, Y. Nagasawa, H. Kandori, A. Douhal, and K. Kemnitz (With 3 Figures)	571
Ultrafast Studies and Simulations on Direct Photoinduced Electron Transfer in the Betaines By A.E. Johnson, N.E. Levinger, G.C. Walker, and P.F. Barbara (With 3 Figures)	576
Picosecond Infrared Study of Ultrafast Electron Transfer and Vibrational Energy Relaxation in $[(\text{NC})_5\text{RU}^{\text{II}}\text{CNRu}^{\text{III}}(\text{NH}_3)_5]^{1-}$ By P.O. Stoutland, S.K. Doorn, R.B. Dyer, and W.H. Woodruff (With 1 Figure)	579
Ultrafast Studies on Intervalence Charge Transfer By K. Tominaga, D.A.V. Kliner, J.T. Hupp, and P.F. Barbara (With 1 Figure)	582
Picosecond Infrared Study of Intramolecular Energy Transfer in $[(\text{phen})(\text{CO})_3\text{Re}^{\text{I}}(\text{NC})\text{Ru}^{\text{II}}(\text{CN})(\text{bpy})_2]^+$ By R.B. Dyer, K.A. Peterson, K.C. Gordon, W.H. Woodruff, J.R. Schoonover, T.J. Meyer, and C.A. Bignozzi (With 1 Figure)	585
Noise-Induced Intramolecular Electron Transfer Processes in Polar Media By P.O.J. Scherer	587
Femtosecond Proton Transfer in the Electronic Ground State of Vibrationally Hot Molecules By T. Elsaesser, W. Frey, and M.T. Portella (With 2 Figures)	589

Solvent Effects on the Fast Proton Transfer of 3-Hydroxyflavone By B.J. Schwarz, L.A. Peteanu, and C.B. Harris (With 3 Figures)	592
Time-Resolved Charge Separation in Acceptor-Substituted Anthrylpolyenes By H. Port, G. Quapil, H.C. Wolf, F. Effenberger, C.-P. Niesert, R. Buhleier, Z. Gogolak, and J. Kuhl (With 2 Figures)	596
Vibrationally Unrelaxed <i>cis</i> -Stilbene Photoproducts Examined Through Two-Color UV Pump-Probe Anti-Stokes Raman Spectroscopy By D.L. Phillips, J.-M. Rodier, and A.B. Myers (With 4 Figures)	598
Vibrational Energy Redistribution and Relaxation in the Photoisomerization of <i>cis</i> -Stilbene By R.J. Sension, S.T. Repinec, A.Z. Szarka, and R.M. Hochstrasser (With 2 Figures)	601
Photoisomerization of <i>cis</i> -Stilbene in Compressed Solvents By L. Nikowa, D. Schwarzer, J. Troe, and J. Schroeder (With 2 Figures)	603
Ultrafast Torsional Dynamics in Adsorbates: An SSHG Study By M.J.E. Morgenthaler and S.R. Meech (With 1 Figure)	606
Barrierless Photochemical Isomerization By U. Åberg, E. Åkesson, I. Fedchenia, and V. Sundström (With 2 Figures)	608
Femtosecond Molecular Dynamics in Liquids By D.A. Wiersma, E.T.J. Nibbering, and K. Duppen (With 4 Figures)	611
Femtosecond Solvent Dynamics Studied by Time-Resolved Fluorescence and Transient Birefringence By S.J. Rosenthal, N.F. Scherer, M. Cho, X. Xie, M.E. Schmidt, and G.R. Fleming (With 2 Figures)	616
Adiabatic and Nonadiabatic Effects in Solvation Dynamics By E. Neria and A. Nitzan (With 1 Figure)	618
Excited-State Processes of 7-Azaindole By M. Négrerie, F. Gai, J.-C. Lambry, J.-L. Martin, and J.W. Petrich (With 1 Figure)	621
Excited-State Proton Transfer and Hydrogen-Bonding Dynamics in 7-Azaindole: Time-Resolved Fluorescence and Computer Simulation By C.F. Chapman, T.J. Marrone, R.S. Moog, and M. Maroncelli	624
Transient Hole Burning Studies of Electronic State Solvation: Phonon and Structural Contributions By J. Yu, J.T. Fourkas, and M. Berg (With 2 Figures)	626

Subpicosecond Study of the Dynamic Processes in Push-Pull Styrenes and the Role of Solvation By P. Hébert, G. Baldacchino, T. Gustavsson, V. Kabelka, P. Baldeck, and J.-C. Mialocq (With 3 Figures)	628
Picosecond Studies of Charge Transfer States in “Push-Pull” Linear Diphenyl Polyenes: Experimental Evidence for TICT and Bicimer States By J.M. Viallet, F. Dupuy, R. Lapouyade, W.Q. Zheng, and C. Rullière (With 2 Figures)	631
Features of the Dual Fluorescence of 4-N,N-dialkylaminoalkylbenzoates in Alkanes By M.C.C. de Lange, D.T. Leeson, A.H. Huizer, and C.A.G.O. Varma (With 1 Figure)	634
Investigation of Fast Relaxation Processes in Non-Fluorescent Rhodamine Dyes By P. Plaza, N.D. Hung, M.M. Martin, Y.H. Meyer, and W. Rettig (With 1 Figure)	636
Femtosecond Photodissociation of Aromatic Disulfides Followed by Solvent Relaxation By N.P. Ernsting (With 4 Figures)	638
Femtosecond Dynamics of C–O Bond Cleavage of a Spirooxazine Photochromic Reaction By N. Tamai and H. Masuhara (With 2 Figures)	641
Dynamics of Molecular Rotation at the Air/Water Interface by Time- Resolved Second-Harmonic Generation By A. Castro, D. Zhang, and K.B. Eisenthal (With 5 Figures)	644
Energy Relaxation and Redistribution in Large Molecules in Solution on Ultrafast Time Scales By C.B. Harris, J.C. King, K.E. Schultz, B.J. Schwartz, and J.Z. Zhang (With 2 Figures)	650
Photodissociation and Recombination Dynamics of I_2^- in Solution By J.C. Alfano, D.A.V. Kliner, A.E. Johnson, N.E. Levinger, and P.F. Barbara (With 3 Figures)	653
Probing the Microscopic Molecular Environment in Liquids with Femtosecond Fourier-Transform Raman Spectroscopy By D. McMorro, S.K. Kim, J.S. Melinger, and W.T. Lotshaw (With 3 Figures)	656
The Homogeneity of Liquid Phase Vibrational Line Broadening from Raman Echo Experiments By L.J. Muller, D. Vanden Bout, and M. Berg (With 2 Figures)	658

Excited State Photoreactions of Chlorine Dioxide in Solution By R.C. Dunn and J.D. Simon (With 2 Figures)	661
Bimolecular Reactions are Power-Full By A. Masad, S.Y. Goldberg, D. Huppert, and N. Agmon (With 4 Figures)	664
Dynamics and Mechanism of Cu-Porphyrin Triplet Quenching Through Liganding by Oxygen-Containing Solvents By V.S. Chirvony and R. Gadonas	667
Fast Processes in Liquid Alkane Photolysis Above the Ionization Threshold By M. Sander, U. Brummund, K. Luther, and J. Troe (With 1 Figure) . . .	669
Index of Contributors	671

Molecular Processes in the Primary Reaction of Photosynthetic Reaction Centers

W. Zinth¹, C. Lauterwasser¹, U. Finkle², P. Hamm¹, S. Schmidt²,
and W. Kaiser²

¹Institut für Medizinische Optik der Universität München,
Barbarastr. 16/IV, W-8000 München 40, Fed. Rep. of Germany

²Physik Department E 11 der Technischen Universität München,
W-8046 Garching, Fed. Rep. of Germany

Abstract: The primary electron transfer is investigated for wildtype reaction centers from *Rhodobacter sphaeroides*, mutant reaction centers and reaction centers with modified bacteriochlorophyll. Experimental results are presented which strongly support the idea that the electron transfer is stepwise involving the accessory bacteriochlorophyll as a real intermediate electron carrier.

1. Introduction

The energy converting processes of bacterial photosynthesis start in a large chromoprotein called reaction center (RC). At first light energy leads to electronic excitation of a chromophore. Subsequently the electronic excitation initiates an electron transfer (ET) via several acceptor molecules. Finally the electron reaches the quinone Q_B . Further secondary transfer processes involve diffusive motion of protons and large organic molecules. Schematically the structural arrangement of the electron carrying pigments in the RC's is shown in Fig. 1 /1, 2/. The pigments are incorporated in two branches (A and B) related by an approximate C_2 symmetry. The two branches cross at two strongly interacting bacteriochlorophyll molecules forming the special pair P which acts as a primary electron donor. Subsequently each branch contains a monomeric bacteriochlorophyll molecule B_A and B_B , a bacteriopheophytin (H_A , H_B) and a quinone (Q_A , Q_B). Various experiments have revealed that the two pigment branches are not equivalent and that the reactive electron transfer uses the A branch.

The very first reaction processes include the initial charge separation and the ET until the bacteriopheophytin H_A . These events take several picoseconds /3-9/. In the next step the electron reaches within approximately 200 ps the quinone Q_A . The secondary quinone Q_B is reduced only much slower on the 10^{-6} s time scale. Transient absorption spectroscopy of the

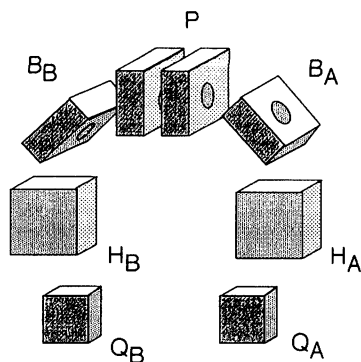


Fig. 1: Schematic of the molecular arrangement of the four bacteriochlorophylls (P, B_A , B_B), the two bacteriopheophytins (H_A , H_B) and the two quinones (Q_A , Q_B) in reaction centers

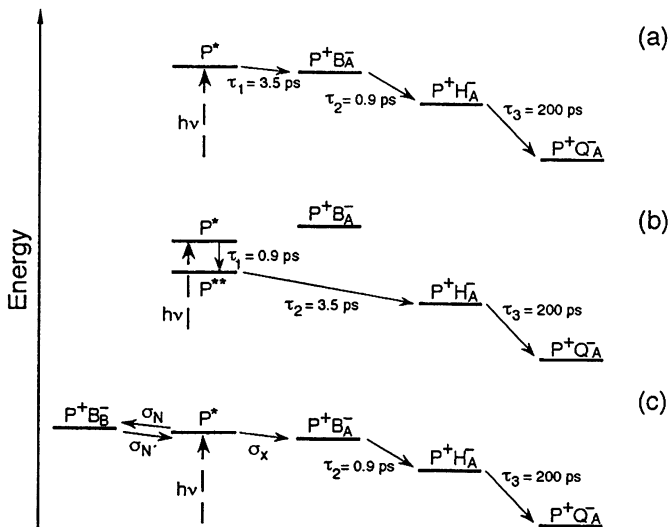


Fig. 2: Reaction models for the primary electron transfer

primary reaction dynamics at room temperature exhibit one time constant around 3.5 ps (in the literature values are reported between 2.8 ps and 4 ps /3-9/) related to the decay of the excited electronic state P^* and a weak subpicosecond kinetic (0.9 ps in Rb. sphaeroides) best seen in the absorption range of the BChl and the BChl anion /7-9/. Until now no generally accepted molecular interpretation of the fast kinetic component exists /10-12/. Two reaction models are currently discussed (see Fig. 2a and b):

The structural arrangement of the reaction centers strongly suggests the stepwise electron transfer model of Fig. 2a: According to this model the electronically excited state P^* of the special pair decays with the time constant of 3.5 ps. Simultaneously an electron is transferred from the special pair to the monomeric bacteriochlorophyll B_A . The second electron transfer is faster and carries the electron with a time constant of 0.9 ps to the bacteriopheophytin H_A . Finally the 200 ps process generates the radical pair $P^+Q_A^-$ where the electron has reached the first quinone.

In model 2b the fast time constant of 0.9 ps is assigned to an excited state relaxation process of the special pair. This process should be vibrational relaxation from the initially populated Franck-Condon-state. In this reaction model the first electron transfer drives the electron with a time constant of 3.5 ps directly to the bacteriopheophytin H_A . This fast long-distance electron transfer is only possible if the monomeric BChl B_A is involved as a virtual intermediate in a superexchange interaction. In this case the energy level of the corresponding radical pair $P^+B_A^-$ is higher than the energy of P^* . From extensive experimental studies the absorption spectra of the different intermediates could be calculated for both models /7-9/. These data were fully consistent with the molecular interpretation of the respective model.

In this paper we will present transient absorption data on RC of Rb. sphaeroides where additional information on the reaction model is obtained by: (i) biochemical modifications of the RC and (ii) changing the temperature of the sample.

2. Results and Discussion

Measurements on low temperature RC are performed on quinone depleted RC from the carotenoid free strain R26.1. The preparation of RC where BChl a at the accessory position B_A is exchanged to approximately 70 % by [3-vinyl]-13²-OH-BChl a is described in Ref. 13. The time resolved absorption experiments are performed using the excite and probe technique with weak subpicosecond pulses (pulse duration \approx 150 fs) generated by a laser-amplifier-system

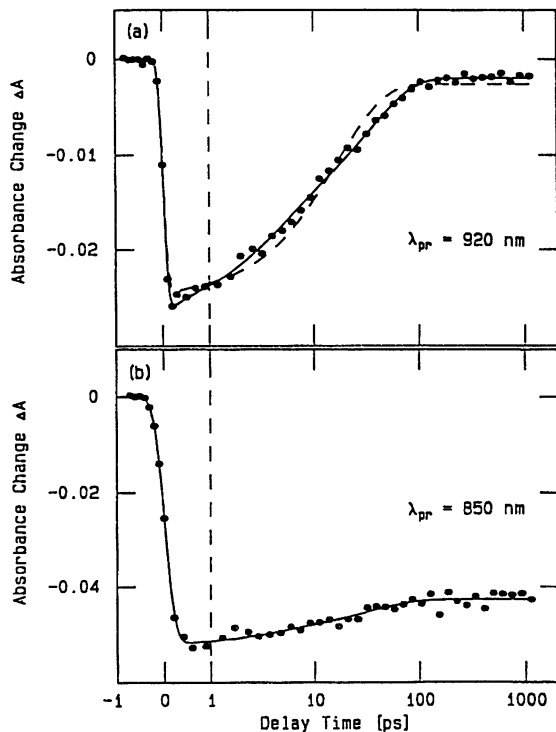


Fig 3: Transient absorption data on [3-vinyl]-13²-OH-RC-preparations. Probing in the gain region at $\lambda = 920$ nm (a) and in special pair absorption band $\lambda = 850$ nm (b)

with a repetition rate of 10 Hz. The temporal width of the instrumental response function is below 300 fs. Details of the experimental system are described in reference /14/.

Upon lowering the temperature of the RC preparation the picosecond kinetics become faster /14, 15/. The decay of the gain having a time constant of around 3.5 ps at room temperature speeds up to 1.4 ps at 25 K. The 0.9 ps kinetic component also accelerates at lower temperatures. At 25 K a value of 0.3 ps is reached. Throughout the whole temperature range from 300 K to 25 K the spectral signature of the fast component does not change.

Experiments on [3-vinyl]-13²-OH-BChl a containing RC's are shown in Fig. 3. The modification due to the 3 vinyl group is expected to change the redox potential of the BChl and the energy of the radical pair state P⁺B⁻. This change should have pronounced consequences on the ET when the accessory BChl B_A is involved. Indeed, one finds a strong slowing down of the decay of P* (see Fig. 3a for a measurement in the gain region). The experimental data indicate that the RC's containing [3-vinyl]-13²-OH-BChl a have a decay time of P* of 32 ps. Fig. 3b, measured at a wavelength where the P absorption is strong, shows a long-lasting bleaching of P. These observations prove that the exchange leads to RC's which are still photochemically active but where the ET-step out of P* is slowed down by a factor of ten. In the [3-vinyl]-13²-OH-BChl a containing RC's the 0.9 ps component is not visible. Experimental indications exist that a related process appears with a longer time constant in the 5 ps domain. The disappearance of the 0.9 ps component can be taken as a strong indication that the 0.9 picosecond process in wildtype RC is not related to vibrational relaxation of P* since P* is unchanged upon modifying B. This finding argues against the superexchange electron transfer of model 2b.

Additional support of the stepwise model of Fig. 2a comes from the low temperature hole-burning experiments where narrow holes related to a $\tau > 1$ ps process are observed. According to these experiments the 0.3 ps process observed in transient absorption spectroscopy can not

be the first reaction. As a consequence the 0.3 ps time constant (and due to the smooth temperature dependence the 0.9 ps time at room temperature) must be related to the second reaction step.

Other important experimental information is obtained from transient absorption spectroscopy of an antenna deficient mutant (strain U43, pTXA6-10) of *Rb. capsulatus*. Here whole chromatophores are investigated instead of isolated RC's. The experiments exhibit the same subpicosecond component as observed in the RC preparation. This finding clearly indicates that the subpicosecond component is not an artefact due to the preparation procedure. Recently emission experiments on RC have shown that the 3.5 ps kinetic component of wildtype RC has to be split into a 2.3 ps and a 7 ps process/17/. Within the scope of the stepwise ET model this biexponentiality can be explained by a transient ET to the accessory bacteriochlorophyll on the B branch as indicated in scheme C of Fig. 2. According to this interpretation the ET on the B branch would be blocked efficiently only between B_B and H_B.

In conclusion, we have shown that the primary processes in photosynthetic RC can be explained by a stepwise electron transfer from the special pair over the different electron carrying pigments. The distance between the pigments is small enough to allow fast and efficient electron transfer in the stepwise model.

Acknowledgement: The author thank H. Scheer and G. Drews for providing us with high quality preparations.

References

1. J.Deisenhofer, H.Michel, *EMBO J.* **8**, 2149 (1989).
2. C.H.Chang, D.Tiede, J.Tang, U.Smith, J.Norris, M.Schiffer, *FEBS Letters* **205**, 82 (1986).
3. N.W.Woodbury, M.Becker, D.Middendorf, W.W.Parson, *Biochem.* **24**, 7516 (1985).
4. J.Breton, J.L.Martin, A.Migus, A.Antonetti, A.Orszag, *Proc. Natl. Acad. Sci. US* **83**, 5121 (1986).
5. J.L.Martin, J.Breton, A.J.Hoff, A.Migus, A.Antonetti, *Proc. Natl. Acad. Sci. US* **83**, 957 (1986).
6. C.Kirmaier, D.Holten, W.W.Parson, *Biochim. et Biophys. Acta* **810**, 49 (1985).
7. W.Holzappel, U.Finkele, W.Kaiser, D.Oesterhelt, H.Scheer, H.U.Stilz, W.Zinth, *Chem. Phys. Letters* **160**, 1 (1989).
8. W.Holzappel, U.Finkele, W.Kaiser, D.Oesterhelt, H.Scheer, H.U.Stilz, W.Zinth, *Proc. Natl. Acad. Sci. US* **87**, 5168 (1990).
9. K.Dressler, E.Umlauf, S.Schmidt, P.Hamm, W.Zinth, S.Buchanan, H.Michel, *Chem. Phys. Letters* **183**, 270 (1991).
10. M.Plato, K.Möbius, M.E.Michel-Beyerle, M.Bixon, J.Jortner, *J. Am. Chem. Soc.* **110**, 7279 (1988).
11. R.A.Marcus, *Chem. Phys. Letters* **133**, 471 (1987).
12. M.Bixon, J.Jortner, M.E.Michel-Beyerle, *Biochim. et Biophys. Acta* **1056**, 301(1991).
13. A. Struck, E. Cmiel, I. Katheder, H. Scheer, *FEBS Lett.* **268**, 180 (1990).
14. C.Lauterwasser, U. Finkle, H. Scheer, W. Zinth; *Chem. Phys. Letters* **183**, 471 (1991).
15. G.R.Fleming, J.L.Martin, J.Breton, *Nature* **333**, 190 (1988).
16. S.G. Johnson, D. Tang, R. Jankowiak, J.M. Hayes, G. J. Small, *J. Phys. Chem.* **93**, 5953 (1989) .
17. P. Hamm, W. Zinth, (1992) same proceedings.